

Dephasing in Rashba spin precession along multichannel quantum wires and nanotubes

Wolfgang Häusler*

*Physikalisches Institut, Albert-Ludwigs-Universität, Hermann-Herder-Straße 3,
79104 Freiburg, Germany*

Coherent Rashba spin precession along interacting multi-mode quantum channels is investigated, revisiting the theory of coupled Tomonaga-Luttinger liquids. We identify susceptibilities as the key-parameters to govern exponents and Rashba precession lengths. In semiconducting quantum wires spins of different transport channels are found to *dephase* in their respective precession angles with respect to one another, as a result of the interaction. This could explain the experimental difficulty to realize the Datta Das transistor. In single walled carbon nanotubes, on the other hand, interactions are predicted to suppress dephasing between the two flavor modes at small doping.

PACS numbers: 71.10.Pm; 71.70.Ej; 72.25.Dc; 73.21.Hb; 73.22.-f

I. INTRODUCTION

Rashba precession¹ of spins and its manipulation has been studied intensively² in recent years, aiming to control the coherent propagation of electron spins. One goal is to realize a spin transistor³; another interesting option could be to switch between singlet and triplet entangled states for directing, for example, noise statistics⁴ or for quantum computing. Despite of major efforts, manipulation of coherent Rashba precession could not be demonstrated experimentally yet in the polarizer-analyzer type transport arrangement. Rashba spin splitting occurs near surfaces in the presence of internal or externally applied symmetry breaking electric fields perpendicular to the transport direction¹. Spins precess when injected out of the spin-orbit eigendirections. Any dephasing along the structure limits successful transistor operation. One important dephasing mechanism in spin-orbit active structures of more than one dimension arises due to momentum randomizing scattering events by impurities (elastically), by phonons (inelastically)⁵, or by electron-electron scattering events⁶. One-dimensional structures confine the direction of propagation, thus reducing this source of dephasing mechanism⁷. Already in their original proposal³ Datta and Das therefore suggested to use clean one-dimensional structures for the spin-orbit active medium. The current work focuses on quantum wires and assumes absence of momentum randomizing scattering events. No spin *relaxing* mechanisms (in the sense that off-diagonal entries of the spin density matrix decay) will be considered here.

Most quantum wires of current experiments accommodate more than one transport channel at the Fermi energy. This holds true also for single walled carbon nanotubes (NT) where at least two flavor channels carry (spin) current. In NT spin transport has been established experimentally⁸ and studied theoretically⁹. Other experimental multichannel systems consist of arrays of quantum wires fabricated artificially in parallel at close proximity¹⁰. In any multichannel wire the interesting question arises whether Rashba spin phases increase by equal amounts along different channels or not. Provided the kinetic energy dispersion is strictly parabolic, described by a common effective carrier mass in each channel as in most semiconducting quantum wires, one would

expect equal spin phases in all channels as a result of the linear splitting by the Rashba energy³, so that their probabilities to enter the spin selective drain contact all add up. We shall demonstrate that Coulomb interactions between charged electrons affect their spin propagation properties and ultimately destroy the phase relationship of Rashba precessing spins between channels in quantum wires (QW) fabricated on the basis of semiconducting material. This limits operation of the Datta Das spin transistor. In metallic single walled nanotubes, on the other hand, with their linear kinetic energy dispersion, spins dephase between modes already without accounting for interactions; remarkably, in this case we find that the Coulomb interaction *suppresses* this single particle dephasing between the two flavor modes, particularly at small doping, thus facilitating coherent spin precession along NT.

II. INTERACTING MULTIMODE QUANTUM WIRES

Before addressing the effect of spin-orbit coupling let us first discuss the (possibly screened) Coulomb interactions within and between transport channels. One-dimensional systems are particularly susceptible to electron-electron interactions, even when weak¹¹. Neither in semiconducting QW¹² nor in NT^{13,14} interactions can be disregarded. Contrary to higher dimensions they show up, for example, as nonuniversal power laws at low energies. The most convenient theoretical framework is the Bosonic Tomonaga-Luttinger liquid (TL)¹⁵ developed since the seminal work by Haldane¹⁶. However, *a priori*, it is not clear in how far the TL-model can be applied to multichannel situations. Strictly equivalent modes of equal particle densities and interaction matrix elements, for example, tend to stabilize a gapped charge or spin density, non-TL low energy phase¹⁷ due to the appearance of relevant (in the sense of a perturbative renormalization group treatment) momentum conserving intermode backscattering processes. On the other hand, most real systems lack such a strict equivalence of modes. In multichannel quantum wires particle densities differ at given Fermi energy, and even systems of Ref. 10 without fine tuning of densities, or the two flavor modes of NT at not exact zero doping cease to be strictly equivalent.

Here, we therefore focus on the generic case of unequal modes which are expected to stay in the gap-less low energy TL phase.

In this phase Matveev and Glazman (MG) have computed a power law for the density of states of spin-less electrons at the end of the n -th mode¹⁸:

$$\nu_n(\omega) \sim \omega^{\beta_n}, \quad (1)$$

generalizing the single channel case^{11,16,19}. MG obtained the exponents β_n within a pure plasmon model by modeling the charge density fluctuations as coupled harmonic strings. Plasmon velocities s_ℓ and the normalized eigenmodes $\gamma_{n\ell}$, as obtained from the dynamical matrix, determine¹⁸

$$\beta_n^{\text{MG}} = -1 + \sum_\ell |\gamma_{n\ell}|^2 s_\ell / v_n, \quad (2)$$

v_n is the Fermi velocity in the n -th channel. This approach merely accounts for long wave length charge properties and can be shown to be equivalent to the random phase approximation (RPA) to plasmon velocities²⁰ generalized to coupled modes²¹. It has been pointed out²² that the RPA result deserves improvement at small particle densities. Moreover, it disregards exchange processes and spin, and tacitly presumes ‘super’ Galilei invariance of every channel individually, as discussed below. Spin properties and exchange are known to depend on short wave length properties of the interaction²³.

For given microscopic interaction the parameters of the single channel TL model, and therewith sound velocities and exponents, have been obtained from homogeneous and static susceptibilities²², exploiting *exact* thermodynamic relations^{16,15,24}. These susceptibilities, in turn, can be computed to high accuracy by standard many-body techniques from the underlying Fermion model, beyond the RPA or perturbative accuracies. This way the asymptotic behavior of correlation functions has been determined in the 1D Hubbard model from the Bethe Ansatz ground state energy E_0 ²⁴. In the Galilei invariant charge sector of QW only the compressibility $\kappa = \left(L \frac{\partial^2 E_0}{\partial N^2}\right)^{-1}$ is required (N is the particle number and L the system length) to fix the exponent parameter $K_\rho = \sqrt{\pi \kappa v_F / 2}$. In spin sector SU(2) spin rotation invariance enforces $K_\sigma = 1$ (cf., e.g., Refs. 15 and 25). As a further important property of one dimension charge and spin density wave excitations are expected to separate and move at different velocities¹⁶. Evidence for this has been found in recent experiment¹⁰. Spin velocities of QW have been deduced from quantum Monte Carlo magnetic susceptibilities²⁶. Here we generalize this *a priori* exact thermodynamic approach to coupled channels. Spins can be incorporated as separate $s = \pm$ modes which allows to account even for non SU(2) invariant situations, as it arises for example in the presence of a Zeeman-field²⁷.

From the microscopic point of view we consider the 1D system

$$H = \sum_{n,k,s} \epsilon_n(k) c_{n,k,s}^\dagger c_{n,k,s} + \frac{1}{2L} \times \sum_{k,s,k',s',q} c_{n_1,k-q,s}^\dagger c_{n_2,k'+q,s'}^\dagger V_{n_1 n_2 n_3 n_4}(q) c_{n_3,k',s'} c_{n_4,k,s}. \quad (3)$$

Fermi annihilation operators $c_{n,k,s}$ refer to wave vector k and spin s of mode n . Assuming electron wave functions of the product form $\sim \varphi_n(x_\perp) e^{ikx} / \sqrt{L}$ (for a discussion of this product assumption cf. Ref. 22) we obtain

$$V_{n_1 n_2 n_3 n_4}(q) = \frac{2e^2}{\varepsilon} \int dx_\perp \int dx'_\perp \times \varphi_{n_1}^*(x_\perp) \varphi_{n_2}^*(x'_\perp) \varphi_{n_3}(x'_\perp) \varphi_{n_4}(x_\perp) K_0(|q||x_\perp - x'_\perp|) \quad (4)$$

from the 3D-Coulomb interaction between electrons, ε is the dielectric constant of the material surrounding the wire. The $V_{n_1 n_2 n_3 n_4}$ can be expressed analytically for many cross sections of physical relevance^{28,29}. Some of the $V_{n_1 n_2 n_3 n_4}$ vanish by symmetry: for example, angular momentum conservation on a cylinder surface of NT requires $n_1 + n_2 = n_3 + n_4$, or $\sum_i n_i$ must be even in QW of mirror symmetric cross section. ‘Direct’ terms may be approximated as $V_{nn'n'n'}^{\text{QW}}(q) \approx \frac{e^2}{\varepsilon} e^{\tilde{q}} K_0(\tilde{q})$ or $V_{nn'n'n'}^{\text{NT}}(q) \approx \frac{2e^2}{\varepsilon} I_0(r|q|) K_0(r|q|)$ at q^{-1} larger than the diameter (QW) d or the radius r (NT). At small q both reveal the same logarithmic increase which eventually will be screened by remote metallic gates. In the above formulae I_ν and K_ν are Bessel functions and $\tilde{q} = d^2 q^2 / 8$. ‘Exchange’ terms between the lowest two modes of parabolically confined QW are $V_{1212}^{\text{QW}}(q) = \frac{e^2}{\varepsilon} \tilde{q} e^{\tilde{q}} (K_1(\tilde{q}) - K_0(\tilde{q}))$ ²⁸ while in NT the two lowest degenerate flavor modes have angular momentum zero and interact $\sim V_{1111}^{\text{NT}}(q)$.

The Boson model¹⁶, describing gapless excitations of Fermions in a 1D wire of length L (periodic boundary conditions) in the vicinity of the Fermi energy, takes the form

$$H = \sum_{q \neq 0} \left(H_q^{(1)} + H_q^{(2)} \right) + \frac{\pi}{4L} \left(\vec{N} \mathbf{v}_N \vec{N} + \vec{J} \mathbf{v}_J \vec{J} \right) \quad (5)$$

when generalized to M modes. Bold letters indicate $M \times M$ matrices and the components of vectors refer to modes $1 \leq n \leq M$. In Eq. (5)

$$H_q^{(1)} = \frac{\pi}{L} \sum_{r=\pm} \vec{\varrho}_r(q) \left(\mathbf{v} + \frac{\mathbf{V}^{(1)}}{\pi} \right) \vec{\varrho}_r(-q) \quad (6)$$

$$H_q^{(2)} = \frac{\pi}{L} \sum_{r=\pm} \vec{\varrho}_r(q) \left(\frac{\mathbf{V}^{(2)}}{\pi} \right) \vec{\varrho}_{-r}(-q)$$

describe excitations of right/left ($r = +/ -$) going Bosonic density fluctuations $\varrho_{rn}(q)$ at wave numbers $q \neq 0$. Topological excitations [last term in Eq. (5)] describe changes in the ground state energy when particles N_n or currents J_n are added to mode n at $q = 0$. This second part of Eq. (5) is important in the present context and is governed by generalized homogeneous and static compressibilities and (Drude) conductivities:

$$(\mathbf{v}_N)_{nn'} = \frac{2L}{\pi} \frac{\partial^2 E_0}{\partial N_n \partial N_{n'}}, \quad \text{and} \quad (\mathbf{v}_J)_{nn'} = \frac{2L}{\pi} \frac{\partial^2 E_0}{\partial J_n \partial J_{n'}}, \quad (7)$$

respectively. They generalize corresponding TL parameters for single channels¹⁵ (E_0 is the ground state energy of the interacting electron system) and govern the complete low energy physics. As in the single channel case¹⁶

\mathbf{v}_N and \mathbf{v}_J are related to the interactions between density fluctuations in Eq. (6), moving in the same

$$\mathbf{V}^{(1)}/\pi = (\mathbf{v}_N + \mathbf{v}_J)/2 - \mathbf{v} \quad (8)$$

or opposite

$$\mathbf{V}^{(2)}/\pi = (\mathbf{v}_N - \mathbf{v}_J)/2 \quad (9)$$

directions, assuming $\epsilon_n(k) = \epsilon_n(-k)$ and thus Fermi velocities $(\mathbf{v})_{nn'} = v_n \delta_{nn'}$ of equal magnitudes at either Fermi point.

Importantly, all entries of \mathbf{v}_N and \mathbf{v}_J are observable, at least *in principle*, and must therefore agree in Bosonic (5) or Fermionic [Eq. (3) together with (7)] representation. This allows deduction $\mathbf{V}^{(1)}$ and $\mathbf{V}^{(2)}$ by standard many-body techniques from the given microscopic interaction (4) through Eqs. (7–9). Therefore \mathbf{v}_N and \mathbf{v}_J (and not exponents as often assumed for single channel quantum wires) are the principle parameters governing the low energy physics in the multichannel case. They establish the quantitative link to the microscopic Fermion model (3). For real quantum wires self-consistent Hartree-Fock^{22,30}, diagrammatic²³, or Monte Carlo techniques²⁶ were used to deduce TL parameters from a microscopic model for electron-electron interaction potential. As a first approach to multichannels we rely on the perturbative approximation below, which, when including the Fock term (as crucial in spin sector), proves already as superior to the often used random phase approximation²⁰ to TL parameters²².

The matrices \mathbf{v}_N and \mathbf{v}_J reflect symmetries of the system under permutations of modes. One important case are equivalent modes when $(\mathbf{v})_{nn'} = v \delta_{nn'}$ in Eq. (6), and \mathbf{v}_N and \mathbf{v}_J both are cyclic matrices. Then Eq. (5) can be diagonalized and the Bogoliubov transformation solving for plasmon velocities and exponents can be carried out separately in each of the resulting independent ‘normal mode’ TL (two equivalent channels, for example, can be separated trivially into independent $\varrho_1 + \varrho_2$ and $\varrho_1 - \varrho_2$ modes). Another symmetry is Galilei invariance (observed in QW and NT) for which $\text{Tr } \mathbf{v}_J = \sum_n v_n$ ³¹ stays independent of interactions. The higher symmetry, where the ground state energy changes only by the trivial kinetic part, independently of the interaction strength, under boosting any individual channel, $J_n \rightarrow J_n + \delta_n$, we call ‘super’ Galilei invariance. It implies $\mathbf{v}_J = \mathbf{v}$, i.e., $\mathbf{V}^{(1)} = \mathbf{V}^{(2)}$ which in general is not observed by Eq. (3) though tacitly assumed often in theoretical work.

Of central importance is the single particle density matrix $\langle \psi_n(x) \psi_{n'}^\dagger(0) \rangle$ which can be evaluated from Eq. (5) using Boson operators $a_{nq} = \sqrt{2\pi/L|q|} \sum_r \Theta(rq) \varrho_{rn}(q)$ with $[a_{nq}, a_{n'q'}^\dagger] = \delta_{nn'} \delta_{qq'}$, generalizing the single channel case^{16,15}. New Boson operators b_{nq} eventually diagonalize $H_q^{(1)} + H_q^{(2)}$. They are obtained via a Bogoliubov transformation reading in the multicomponent case $\begin{pmatrix} \tilde{a}^\dagger \\ \tilde{a} \end{pmatrix} = \begin{pmatrix} \mathbf{u} & \mathbf{v} \\ \mathbf{v} & \mathbf{u} \end{pmatrix} \begin{pmatrix} \tilde{b}^\dagger \\ \tilde{b} \end{pmatrix}$. Here, the $M \times M$ matrices \mathbf{u} and \mathbf{v} must satisfy $(\mathbf{w}[\mathbf{u}\mathbf{v}\mathbf{v}^{-1}(\mathbf{w}\mathbf{v}\mathbf{v}^{-1})^\dagger - \mathbf{v}(\mathbf{w}\mathbf{v})^\dagger])\mathbf{w} = \delta_{ll'}$ where $\mathbf{w} = (\mathbf{v}\mathbf{v}^{-1}\mathbf{u} - \mathbf{v}^2)^{-1}$ and \dagger indicates the transpose. This condition is fulfilled when

$$\mathbf{u} = \mathbf{R} \mathbf{c} \mathbf{R} \quad \text{and} \quad \mathbf{v} = \mathbf{R} \mathbf{s} \mathbf{R}, \quad (10)$$

provided \mathbf{R} is orthogonal, and $\mathbf{c}_{ll'} = \delta_{ll'} \cosh \vartheta_l$ and $\mathbf{s}_{ll'} = \delta_{ll'} \sinh \vartheta_l$ are diagonal matrices, $1 \leq l, l' \leq M$. The $\frac{1}{2}M(M-1)$ real parameters of \mathbf{R} and the M angles ϑ_l are found from the $\frac{1}{2}M(M+1)$ equations

$$(\mathbf{c} \quad \mathbf{s}) \begin{pmatrix} \tilde{\mathbf{V}}^{(2)}/\pi & \tilde{\mathbf{v}} + \tilde{\mathbf{V}}^{(1)}/\pi \\ \tilde{\mathbf{v}} + \tilde{\mathbf{V}}^{(1)}/\pi & \tilde{\mathbf{V}}^{(2)}/\pi \end{pmatrix} \begin{pmatrix} \mathbf{c} \\ \mathbf{s} \end{pmatrix} = 0. \quad (11)$$

Here, the tilde connotes rotated symmetric matrices, $\tilde{\mathbf{A}} = \mathbf{R}^{-1} \mathbf{A} \mathbf{R} = \tilde{\mathbf{A}}^\dagger$.

Finally, the M eigenvalues of

$$(\mathbf{c} \quad \mathbf{s}) \begin{pmatrix} \tilde{\mathbf{v}} + \tilde{\mathbf{V}}^{(1)}/\pi & \tilde{\mathbf{V}}^{(2)}/\pi \\ \tilde{\mathbf{V}}^{(2)}/\pi & \tilde{\mathbf{v}} + \tilde{\mathbf{V}}^{(1)}/\pi \end{pmatrix} \begin{pmatrix} \mathbf{c} \\ \mathbf{s} \end{pmatrix}, \quad (12)$$

with the outcome of Eq. (11) inserted for \mathbf{c} , \mathbf{s} , and \mathbf{R} , are the (generalized) plasmon velocities of $\sum_{q \neq 0} (H_q^{(1)} + H_q^{(2)})$. The same sequence of transformations does not, in general, diagonalize the topological excitations which explains why coupled TLs cannot necessarily be decomposed into independent ‘normal mode TLs’.

Equations (7–12) allow to calculate the (asymptotic) power law behavior of any Fermion function, cf. Eq. (18) below. This completes the solution for low energy properties in multi-mode electron liquids in 1D. In the (super-Galilei invariant) special case, $(\mathbf{V}^{(1)})_{nn'} = (\mathbf{V}^{(2)})_{nn'} = V_0$ for all n and n' , the ensuing open boundary exponent as well as the plasmon velocities Eq. (12) agree with the results of Ref. 18. As stated above, the present approach includes spins through separate modes $s = \pm 1$.

With SU(2) spin rotation invariance charge-spin separation continues to occur in multichannel systems, so that introducing the additional index $\nu = \rho, \sigma$ for the charge and spin sector, respectively, renders \mathbf{v}_N and \mathbf{v}_J block diagonal. Furthermore, the chiral SU(2) \times SU(2) symmetry of the fermionic model at low energies provides separate spin rotation invariance of right and left movers, giving rise to $\mathbf{v}_{N\sigma} = \mathbf{v}_{J\sigma}$ in spin sector. Very strong spin-orbit coupling will spoil charge-spin separation in general. In QW, however, charge and spin are mixed only to the order $\mathcal{O}(\alpha^5)$ ³² which therefore is rarely expected to be of importance [cf. Eq. (13) below, α is the spin-orbit coupling parameter]. In NT, on the other hand, charge-spin separation is already broken to the order $\mathcal{O}(\alpha)$. Here, the very small value of α , expected from the small carbon mass, leaves this breaking less important and justifies calculating Rashba precession lengths to the leading order in α . With charge-spin separation Rashba precession is controlled solely by the spin sector $\nu = \sigma$ where, from now on, the index n runs only over M spatial modes.

III. RASHBA SPIN PRECESSION LENGTH

We address the physical situations referred to in the Introduction by studying two model systems: QW for quantum wires and NT for nanotubes. In QW the single particle kinetic energy dispersion may be regarded as $\epsilon_n^{\text{QW}}(k) = \epsilon_n + k^2/2m_e$ where ϵ_n are subband energies and m_e is the effective mass. The Rashba spin-orbit energy

$$H^{\text{so}} = \alpha(\sigma_x k_z - \sigma_z k) , \quad (13)$$

deemed as independent of the mode index, adds a linear contribution $\pm\alpha k$ and splits $\epsilon_n^{\text{QW}}(k)$ into two equal parabolas intersecting at the origin (this statement holds strictly true only for not unrealistically strong spin orbit coupling strengths, $\alpha \ll v_n$, as discussed above^{32,33}). Both branches are indexed by the electron spin projection perpendicular to the wire axes, taken as the z -direction for convenience (the x -axes points along the wire). Within each mode, at the Fermi energy, the spin splitting yields a finite difference of Fermi momenta $k_{n\uparrow} - k_{n\downarrow} = 2\alpha m_e$ which, as important property of the QW case, does not depend on n . Spins initially polarized along the x -axes therefore precess once over a length $4\pi/|k_{n\uparrow} - k_{n\downarrow}| = 2\pi/\alpha m_e$, equal in all channels.

The other system we consider are metallic carbon nanotubes (NT). Here, spin-orbit coupling³⁴ arise predominantly from the curvature of the tube surface, cf. Ref. 35; in flat graphite layers it vanishes by mirror symmetry. The kinetic energy dispersion may be taken as $\epsilon_n^{\text{NT}}(k) = \pm\{\epsilon_n + v_F[|k_F - k|\Theta(k) + |k_F + k|\Theta(-k)]\}$, disregarding, for simplicity, parabolic parts of the dispersion close to the subband bottoms at ϵ_n . Here, k_F denotes the Fermi momentum at zero doping and v_F the Fermi velocity. For every n there exist two different flavor branches $b = \pm 1$, depending on the magnitude $|k| \gtrless |k_F|$, of opposite velocities at given sign of k . Adding \tilde{H}^{so} from Eq. (13) yields differences $k_{n\uparrow} - k_{n\downarrow} = 2\alpha(\epsilon_F - \epsilon_n + bv_F k_F)/(v_F^2 - \alpha^2)$ at the Fermi energy, and therefore Rashba precession lengths, depending now on n and, additionally, on b .

So far we considered independent electrons for QW and NT. It has been shown recently that electron-electron interactions influence and actually enhance Rashba precession in 2D structures³⁶ and in single transport channels³². To calculate Rashba lengths on the basis of the multi channel TL model (5) requires expressing Eq. (13) in Bose variables. As in single channels³² H_{so} is found to be proportional to the spin currents $J_{n,\sigma}$. The expressions

$$H_{\text{so}}^{\text{QW}} = -\alpha m_e \sum_n v_n J_{n,\sigma} \quad (14)$$

and

$$H_{\text{so}}^{\text{NT}} = -\alpha v_F \sum_{\substack{n \\ \epsilon_n < |\epsilon_F|}} \frac{\epsilon_F - \epsilon_n + bv_F k_F}{v_F^2 - \alpha^2} J_{n,\sigma} , \quad (15)$$

however, differ in the two cases, QW and NT, as can be checked in the limit of vanishing interaction, when $(\mathbf{v}_{\text{N}\sigma})_{nn'} = (\mathbf{v}_{\text{J}\sigma})_{nn'} = v_n \delta_{nn'}$ in Eq. (5) reproduces the Rashba precession lengths $2\pi/|k_{n\uparrow} - k_{n\downarrow}|$ in individual QW or NT channels, respectively (H_{so} is a single particle operator and does not depend on the Coulomb interaction).

With Eqs. (14) or (15) we are now in the position to calculate

$$f(L) = \frac{1}{M} \sum_{nn'} \langle (\psi_{n\uparrow}(L) + \psi_{n\downarrow}(L)) (\psi_{n'\uparrow}^\dagger(0) + \psi_{n'\downarrow}^\dagger(0)) \rangle , \quad (16)$$

employing the well known Boson representation for Fermi operators $\psi_{ns}(x)$ ¹⁶. In the spirit of the Datta-Das setup³ the quantity $f(L)$ can be interpreted as the probability amplitude to measure an electron at $x = L$ with its initial spin polarization parallel to the x -axes, provided it was injected at $x = 0$ with equal probability amplitudes into all occupied channels. The result can be represented as

$$f(L) = \sum_{nn'} g_{nn'}(L) \cos(\pi L/\lambda_n) . \quad (17)$$

As indicated in the previous section the asymptotic power law decay of the two point function $g_{nn'}(x) \sim |x|^{-\beta_{nn'}}$ can be expressed through the solutions of Eq. (11) for \mathbf{R} and $\vec{\vartheta}$:

$$\beta_{nn'} = \delta_{nn'} + 2 \sum_j R_{nj} R_{n'j} \sinh^2 \vartheta_j . \quad (18)$$

Equation (18) generalizes the known result for the electron Green function of single channels^{11,16}. By virtue of conformal invariance the time dependence can be deduced, yielding the open boundary exponent

$$\beta_n = -1 + \sum_{n'} R_{nn'}^2 e^{-2\vartheta_{n'}} \quad (19)$$

for the density of states [Eq. (1)].

Equation (17) allows to read off the inverse precession lengths

$$\frac{1}{\lambda_n^{\text{QW}}} = \frac{\alpha m_e}{\pi} \sum_{n'} (\mathbf{v}_{\text{J}\sigma}^{-1})_{nn'} v_{n'} \quad (20)$$

and

$$\frac{1}{\lambda_n^{\text{NT}}} = \frac{\alpha v_F}{\pi} \sum_{\substack{n' \\ \epsilon_{n'} < |\epsilon_F|}} (\mathbf{v}_{\text{J}\sigma}^{-1})_{nn'} \times \frac{\epsilon_F - \epsilon_{n'} + bv_F k_F}{v_F^2 - \alpha^2} , \quad (21)$$

after which spins reverse their polarization in channel n . We see that the λ_n are governed by the matrices $\mathbf{v}_{\text{J}\sigma}$ of spin conductivities. Without electron-electron interaction $(\mathbf{v}_{\text{N}\sigma})_{nn'} = (\mathbf{v}_{\text{J}\sigma})_{nn'} = v_n \delta_{nn'}$ so that $\lambda_n^{\text{QW}} = \lambda$ stay equal in all channels of QW [Eq. (20)]. This would yield optimum transistor operation as discussed before. Interactions, however, alter the diagonal entries and, additionally, generate off-diagonal entries in $\mathbf{v}_{\text{J}\sigma}$, describing the coupling between channels. In general λ_n^{QW} become n -dependent so that different channels dephase. Remarkably, as demonstrated now, interactions *reduce* spin dephasing in the two lowest flavor modes of single walled NT [Eq. (21)], compared to its magnitude in the absence of interactions.

IV. PERTURBATIVE ESTIMATE

Sufficiently weak interactions can justify the perturbative estimate to $\mathbf{v}_{\text{J}\sigma}$. Crucial is the magnitude of nonzero Fourier components, which even in metallic NT are small compared to the Fermi velocity, since the (large) $q = 0$

component of the interaction does not affect the spin sector and is properly accounted for on the RPA level. Imposing SU(2) symmetry [naive low order perturbation theory violates SU(2) invariance²²] results in

$$\begin{aligned}
 (\mathbf{v}_{N\sigma})_{nn'} &= (\mathbf{v}_{J\sigma})_{nn'} = [v_n - \{V_{nnnn}(2k_n) \\
 &+ \sum_{j \neq n} V_{njnj}(k_n + k_j) - V_{njnj}(k_n - k_j)\}/2\pi]\delta_{nn'} \\
 &- [V_{nn'nn'}(k_n - k_{n'})/2\pi](1 - \delta_{nn'}).
 \end{aligned} \quad (22)$$

Here, k_n denotes the Fermi momentum of mode n ³⁷.

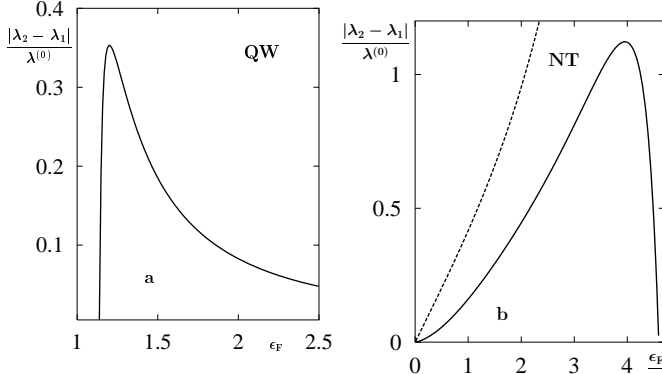


FIG. 1. Difference $|\lambda_2 - \lambda_1|/\lambda^{(0)}$ versus Fermi energy ϵ_F/ω_0 in units of the subband energy ω_0 for two channels, cf. main text. In QW (a) interactions always cause dephasing between both modes while in single walled NT (b) dephasing between the two flavor modes can be significantly suppressed at small doping compared to the noninteracting case (dashed).

Figure 1(a) shows the resulting difference $|\lambda_2 - \lambda_1|/\lambda^{(0)}$ of Rashba lengths relative to this length $\lambda^{(0)}$ in the absence of interactions in a two-channel QW of width $d = a_B/\sqrt{2}$ (a_B is the Bohr radius). This phase difference can exceed 30% and decreases only when ϵ_F and the carrier density increase so that the interaction strength diminishes. We see that dephasing never vanishes within the regime of validity of the perturbational approach at not too small carrier densities in the second subband, $\epsilon_F \gtrsim 1.15\omega_0$ [note that for harmonic confining potential the third subband (not included here) becomes occupied above $\epsilon_F/\omega_0 > 2$]. Experimentally, it might be possible to disentangle two Rashba periods and thus, by monitoring their dependence on the interaction strength (carrier density), verify the predicted dephasing mechanism when two channels are occupied. For the Datta-Das transistor based on semiconductor QWs this result clearly suggests to use only the lowest subband.

In Figure 1(b) the difference of Rashba lengths of the two lowest (degenerate) flavor modes of metallic single wall arm chair (m, m) NT is seen for $m = 5$ [subband energies $\epsilon_1 = \epsilon_2 = 0$, the Fermi momenta $k_{\{2\}} = m/\sqrt{3}r \pm \epsilon_F/v_F$, r is the tube radius, and $e^2/\epsilon v_F \approx 2.7$ ¹⁴], relative to the splitting $\lambda^{(0)}$ at zero doping. Dephasing can be suppressed logarithmically $\sim \epsilon_F/[c_1 - c_2 \ln(\epsilon_F/\omega_0)] + \mathcal{O}(\epsilon_F^3)$ at small doping (c_1 and c_2 depend on the tube radius and c_2 vanishes with the interaction), compared to the interaction free case (dashed) where $c_1 = m/2$. This suggests the use of single walled NT close to the neutrality point³⁸ for coherent Rashba precession along both flavor channels³⁹.

V. SUMMARY

We have calculated Rashba spin precession lengths λ_n in multimode quantum wires, accounting for electron-electron interactions, using the Bosonization method. To this end we have developed an in principle exact description for the TL phase of coupled quantum channels that allows the inclusion spin. Generalized charge and spin compressibilities and conductivities are identified as the key parameters to determine the power law exponents and to establish quantitative contact with the underlying interacting electron model. In semiconducting wires, characterized by a parabolic kinetic energy dispersion, we find that the λ_n become n -dependent, giving rise to doubts whether multichannel systems can be used as active part of the Datta-Das transistor. This result could explain the up to date lack of successful transistor operation and clearly suggests to use single channel quantum wires. In metallic single walled carbon nanotubes, on the other hand, we find that dephasing between the two flavor modes, arising due to the linear kinetic energy dispersion, is suppressed by the electron-electron interaction, particularly at small doping, which could make these systems interesting for coherent spin transport.

I thank Hermann Grabert for many useful conversations. This work has been partly supported by the DFG under SFB 276.

* Present address: Universität Siegen, Fachbereich 7 (Physik), ENC, 57068 Siegen, Germany.

¹ E.I. Rashba, Sov. Phys. Solid State **2**, 1109 (1960); Yu.A. Bychkov and É.I. Rashba, JETP Lett. **39**, 78 (1984).

² J. Nitta, T. Akazaki, H. Takayanagi, and T. Enoki, Phys. Rev. Lett. **78**, 1335 (1997); G. Engels, J. Lange, T. Schäpers, and H. Lüth, Phys. Rev. B **55**, 1958 (1997); T. Schäpers, G. Engels, J. Lange, T. Klocke, M. Hollfelder, and H. Lüth, J. Appl. Phys. **83**, 4324 (1998); C.-M. Hu, J. Nitta, T. Akazaki, H. Takayanagi, J. Osaka, P. Pfeffer, and W. Zawadzki, Phys. Rev. B **60**, 7736 (1999); T. Matsuyama, R. Kürsten, C. Meißner, and U. Merkt, Phys. Rev. B **61**, 15588 (2000).

³ B. Datta and S. Das, Appl. Phys. Lett. **56**, 665 (1990).

⁴ J.C. Egues, G. Burkard, and D. Loss, Phys. Rev. Lett. **89**, 176401 (2002).

⁵ M.I. D'yakonov and V.I. Perel', Sov. Phys. Solid State **13**, 3023 (1972).

⁶ M.Q. Weng and M.W. Wu, Phys. Rev. B **68**, 75312 (2003).

⁷ S. Pramanik, S. Bandyopadhyay, and M. Cahay, Appl. Phys. Lett. **84**, 266 (2004) and cond-mat/0403021 (unpublished).

⁸ K. Tsukagoshi, B.W. Alphenaar, and H. Ago, Nature (London) **401**, 572 (1999); J.-R. Kim, H.M. So, J.-J. Kim, and J. Kim, Phys. Rev. B **66**, 233401 (2002); B. Zhao, I. Mönch, H. Vinzelberg, T. Mühl, and C.M. Schneider, Appl. Phys. Lett. **80**, 3144 (2002).

⁹ L. Balents and R. Egger, Phys. Rev. B **64**, 035310 (2001).

¹⁰ O.M. Auslaender, A. Yacoby, R. de Picciotto, K.W. Baldwin, L.N. Pfeiffer, and K.W. West, *Science* **295**, 825 (2002); Y. Tserkovnyak, B.I. Halperin, O.M. Auslaender, and A. Yacoby, *Phys. Rev. B* **68**, 125312 (2003); U. Zülicke and M. Governale, *Phys. Rev. B* **65**, 205304 (2002).

¹¹ I.E. Dzyaloshinskii and A.I. Larkin, *Sov. Phys. JETP* **38**, 202 (1974).

¹² O.M. Auslaender, A. Yacoby, R. de Picciotto, K.W. Baldwin, L.N. Pfeiffer, and K.W. West, *Phys. Rev. Lett.* **84**, 1764 (2000); M. Rother, W. Wegscheider, R.A. Deutschmann, M. Bichler, and G. Abstreiter, *Physica E* (Amsterdam) **6**, 551 (2000).

¹³ M. Bockrath, D.H. Cobden, J. Lu, A.G. Rinzler, R.E. Smalley, L. Balents, and P.L. McEuen, *Nature* (London) **397**, 598 (1999).

¹⁴ R. Egger and A.O. Gogolin, *Eur. Phys. J. B* **3**, 281 (1998).

¹⁵ See, for example, J. Voit, *Rep. Prog. Phys.* **58**, 977 (1995).

¹⁶ F.D.M. Haldane, *J. Phys. C* **14**, 2585 (1981).

¹⁷ See, for example, A.M. Finkel'stein and A.I. Larkin, *Phys. Rev. B* **47**, 10461 (1993); H.J. Schulz, *Phys. Rev. B* **53**, R2959 (1996); O.A. Starykh, D.L. Maslov, W. Häusler, and L.I. Glazman, *Gapped phases of quantum wires*, in 'Low-Dimensional Systems – Interactions and Transport Properties', ed. by T. Brandes, Lecture Notes in Physics, Springer (2000), p. 37, cf. also cond-mat/9911286; Ref. 14. In the present work we call the individual 1D system interchangeably 'mode' or 'channel'.

¹⁸ K.A. Matveev and L.I. Glazman, *Phys. Rev. Lett.* **70**, 990 (1993).

¹⁹ C.L. Kane and M.P.A. Fisher, *Phys. Rev. Lett.* **68**, 1220 (1992).

²⁰ Q.P. Li, S. Das Sarma, and R. Joynt, *Phys. Rev. B* **45**, 13713 (1992).

²¹ W. Häusler, (unpublished).

²² W. Häusler, L. Kecke, and A.H. MacDonald, *Phys. Rev. B* **65**, 085104 (2002).

²³ L. Calmels and A. Gold, *Europhys. Lett.* **39**, 539 (1997); L. Kecke and W. Häusler, *Phys. Rev. B* **69**, 085103 (2004).

²⁴ H.J. Schulz, *Phys. Rev. Lett.* **64**, 2831 (1990).

²⁵ T. Giamarchi, *Quantum Physics in One Dimension* (Clarendon, Oxford 2004).

²⁶ C.E. Creffield, W. Häusler, and A.H. MacDonald, *Europhys. Lett.* **53**, 221 (2001).

²⁷ T. Kimura, K. Kuroki, and H. Aoki, *Phys. Rev. B* **53**, 9572 (1996).

²⁸ G.Y. Hu and R.F. O'Connell, *Phys. Rev. B* **42**, 1290 (1990).

²⁹ E.G. Mishchenko, A.V. Andreev, and L.I. Glazman, *Phys. Rev. Lett.* **87**, 246801 (2001).

³⁰ W. Häusler and A.H. MacDonald, *J. Phys. Soc. Jpn. Suppl.* **A 72**, 195 (2003).

³¹ This property is related with conductance quantization of ballistic wires.

³² W. Häusler, *Phys. Rev. B* **63**, 121310 (2001).

³³ W. Häusler, *Physica E* (Amsterdam) **18**, 337 (2003).

³⁴ A. De Martino, R. Egger, K. Hallberg, and C.A. Balseiro, *Phys. Rev. Lett.* **88**, 206402 (2002).

³⁵ M.V. Entin and L.I. Magarill, *Phys. Rev. B* **64**, 085330 (2001).

³⁶ G.-H. Chen and M. E. Raikh, *Phys. Rev. B* **60**, 4826 (1999).

³⁷ Interactions may redistribute carriers between the channels for the ground state; here, $2k_n/\pi$ is the carrier density as measured in channel n after this relaxation has taken place. Additional redistribution due to H_{so} is negligible.

³⁸ Precisely at zero doping, however, small energy gaps are dynamically generated in spin sector¹⁴ which suppress Rashba precession. For a recent discussion of this issue cf. A.A. Nerseyan and A.M. Tsvelik, *Phys. Rev. B* **68**, 235419 (2003); ϵ_F should still be larger than these gaps.

³⁹ When doping occupies excited angular momentum states, as often in multi-walled NT, we expect similar dephasing as in quantum wires.